DOI: https://doi.org/10.31351/vol34iss4pp197-214

Formulation, Statistical Optimization and In Vitro Evaluation of Transdermal Anastrozole Nanospanlastic

Laila A. Alwan [*,1] and Shaimaa Nazar Abd Alhammid [2]

[1] Ministry of Health, Diyala Health Department, Baghdad, Iraq.

[2] Department of Pharmaceutics, College of Pharmacy, University of Baghdad, Baghdad, Iraq.

***Corresponding Author**

Received 23/5/2025, Accepted 12 /11/2024, Published 20/12/2025

Abstract

In postmenopausal women, anastrozole reduces estrogen levels, which may inhibit the development of certain breast cancers that depend on high estrogen levels in the body. Anastrozole suffered a first-pass effect, poor aqueous solubility, and gastrointestinal issues. Additionally, improving skin permeability, controlling drug release, and shielding sensitive molecules from deterioration are just a few of the uses for nanoparticles that are gaining popularity. Spanlastics are elastic, malleable nanovesicles based on surfactants. They comprise an edge activator and a nonionic surfactant. In this study, anastrozole nanospanlastic was created to improve patient compliance and control anastrozole transdermal distribution as an alternative to the oral route. Therefore, the study aimed to develop a formulation that could get around these problems by using the advantages of the transdermal administration route and nanotechnology concepts. Minimized sizes with higher zeta potential anastrozole spanlastics were formulated using a response-surface randomized User-Defined method. In addition to one category component that addresses the kind of edge activator, two numerical variables were examined: Span 60 to edge activator ratio (w/w) and sonication duration (min). Zeta potential (mV) and particle size (nm) were investigated as responses. A mathematical optimization technique was used to forecast the optimal variable values. With a sonication period of 5 min., the optimized formulation with a Span 60: sodium deoxycholate ratio of 9:1 w/w revealed particle dimensions of 138 nm with a zeta potential of -32 mV. Formula (F2) was seen using transmission electron microscopy to have a homogeneous and spherical shape. Because of its tiny particle size, high entrapment efficiency percentage (80.2 ± 4.3%), and 12-hour release pattern, formula (F2) was selected. The compatibility study did not reveal any interaction of anastrozole with other components. The previously described findings suggest spanlastics may be potentially effective drug carriers for transdermal medication administration.

Keywords: Anastrozole, Edge Activator, Nanospanlastic, Surface Randomized Design, Transdermal

Introduction

Anastrozole (Ana) is a third-generation aromatase inhibitor used as an adjuvant treatment for hormone receptor-positive breast cancer [(1,2)]. Menopausal and postmenopausal females have a higher incidence of developing breast cancer than younger women, with the incidence of the disease rising with age [(3,4)]. Since estrogen is the main mitogen, hormonal modulation is an effective therapy in cases where one-third of breast cancers are hormone-dependent [(5,6)]. Estrogen and progesterone receptors are markers for tumours that can reply to endocrine treatment [(7,8)]. Inhibiting the synthesis of estrogen in postmenopausal women with metastatic breast cancer may be achieved by aromatase inhibition by using the nonsteroidal inhibitor anastrozole (Arimidex®) [(9,10)]. Compared to other endocrine therapies, aromatase inhibition has several advantages, such as a familiar action device, selective reduction of estrogen combination, absence of estrogenic side effects, and lack of cross-resistance to antiestrogens [(11,12)].In contrast to other aromatase inhibitors, anastrozole offers several benefits, such as a favourable safety profile, high effectiveness and specificity used for the aromatase enzyme, ease of administration, and no requirement for corticosteroid replacement [(13,14)]. In 2003, women who had experienced menopause and were at a high risk of developing breast cancer were recruited for the International Breast Cancer Intervention Study II. They were given either a comparable placebo or one milligram of anastrozole daily. Following a median follow-up of sixty months, the first study discovered a fifty-three per cent decrease in the overall incidence of breast cancer [(15, 16)]. Made of sorbitan esters (Spans) and nonionic surfactants, spanlastics are innovative elastic nano vesicular [(17,18,19)]. Because of its lipophilic nature with saturated alkyl chains, span 60 is the most excellent, widely cast-off version of Spans. Edge activators (EA) are another component

of spanlastics that enhance vesicle fluidity, deformability, and compositional absence of cholesterol. Owing to their unique ability to increase penetration, spanlastics provide a novel mode of administration wherein integral vesicles may pass the biological membrane barriers, permitting medications to be applied topically and noninvasively to various tissues [19,20,21].

Spanlastics, enclosed by a compartment of internal hydrophilic and outward lipophilic layers, may provide hydrophilic and hydrophobic medications. Spanlastics are non-toxic, biodegradable, and non-immunogenic vesicular carriers. Numerous studies have shown that using spanlastics may significantly improve patient compliance, boost medicine absorption, improve therapeutic efficacy, and decrease adverse effects [20,21]. Also, an edge activator breaks down the lipid membrane of the nanovesicles, increasing their permeability and deformability via biological membranes [22,23]. Recently, interest has been resurgent in using spanlastics to improve medication administration. To possibly enhance ciprofloxacin trans-tympanic delivery, Al-Mahallawi *et al* produced Nano-spanlastics [24]. Another study produced a successful spanlastics carrier encapsulated in clotrimazole. This formulation treats fungal keratitis by delivering clotrimazole via the eyes with improved antifungal activity [25].Moreover, spanlastics nanovesicles loaded with terbinafine hydrochloride enhanced drug penetration through the nails, suggesting that spanlastics might be used for terbinafine hydrochloride delivery [26]. To treat arthritis, spanlastics have been used to supplement topical fenoprofen calcium delivery, leading to a longer-lasting and better anti-inflammatory effect [27]. Based on prior studies, this study combines the advantages of spanlastics dispersion with the promise of nanotechnology to improve anastrozole delivery. The study aimed to raise the zeta potential and reduce particle size.

Materials and Methods

Material

Anastrozole is purchased from Qingdao-Sigma Chemical Co., Ltd. (Qingdao, China). Sigma-Aldrich Chemie GmbH (Taufkirchen, Germany) provided the remaining ingredients, including Span® 60, Tween® 80, sodium deoxycholate (SDC), buffer solution and analytical solvents. All other equipment and instruments were obtained locally.

Methods

Method of preparation of Ana-SPLs

The ethanol injection technique created the Ana-SPLs. Anastrozole (10 mg) and the predetermined amounts of Span 60 and Ana were dissolved in 10 mL of absolute ethanol. After that, the ethanolic solution was slowly injected into 10 ml of heated water solution (60 °C) that contained an edge activator. With 250 mg, the span-to-edge activator ratio was determined using their corresponding ratios following the experimental design. The mixture was stirred at 1000 rpm for forty-five minutes to allow the organic solvent to evaporate. A dispersion was produced and ultrasonically agitated for 5 minutes or not (as stated in the experimental design); after that, the volume was adjusted to 10 mL [28,29]. Furthermore, Ana was suspended in an aqueous dispersion of 0.5% sodium carboxymethyl cellulose and stirred at 400 rpm with a magnetic stirrer to create a raw Ana suspension for the comparison with Ana-SPLs released investigation.

Characterization Ana-SPLs

Determination of vesicle size (Ps) and zeta potential (Zp)

Using a Zetasizer (Malvern Panalytical Ltd., Malvern, UK), the prepared Ana-SPLs were characterized for particle size (z-average) and zeta potential. The samples were suitably diluted before testing. Zeta potential was determined by tracking the colloidal nanospanlastic vesicles' electrophoretic movement in an electrical field [30]. Three duplicates of each measurement were made.

Optimization of Ana-SPLs

Optimization and desirability function approaches were analyzed by yielding the smallest particle size and the most significant zeta potential. The optimized Ana-SPLs were further characterized.

Measuring entrapment percentage

Entrapment percentage (EE%) was examined through an indirect method. After being diluted with water, the adjusted Ana-SPLs were centrifuged for 45 minutes at 10000 rpm. After collecting the aqueous supernatant, the content was measured at 215 nm, which was the λ max of the drug using a UV analytical method [31]. By using Equation (1), the EE% of Ana in the optimized Ana-SPLs was estimated. EE%= (Ana amount initially added - Ana amount in the supernatant)/ (Ana amount originally added) x100% (1)

In -vitro release profile from Ana-SPLs:

A delivery system's optimal working circumstances and expected *in vivo* efficacy may be reasonably predicted by its *in vitro* release profile [32]. The cumulative percentage of Ans released over time from the formulations was computed for further comparison with Ana suspension. Dissolution profiles for Ana-SPLs were explored. One millilitre of Ana-SPLs dispersion, equivalent to 1 mg of Ana, was placed in modified Franz diffusion cells filled with release media (phosphate buffer saline pH 7.4) for 12 h and tied closed the open ends of the sac to prevent Ana loss. The sac was placed in 250 mL of dissolving media. The temperature of the medium was kept at 37±0.5 °C. During the experiment, 3 mL was removed from the release medium and substituted with a fresh medium to keep the sink

condition at regular time intervals up to 12 h. The collected 3mL was filtered with a 0.22µm syringe filter and spectrophotometrically evaluated at λmax of Ana (215nm). The total quantity of drugs released was computed. The provided results are the average of three replicates [33,34,35]. The same procedure will be repeated for Ana's suspension, and a comparison will be performed between them.Several mathematical models, including zero-order, first-order, Higuchi diffusion model, the Korsmeyer-Pappas, and the Hixson Crowell equation, were used to analyze the drug release data to identify the proper kinetic model and the mechanism underlying the *in vitro* release of Ana from the nanospanlastics. The higher significant coefficient of determination value (R^2) showed the medication's release order [36,37].

Morphology characteristic of the optimized Ana-SPLs:

The optimal Ana-SPL was examined using a transmission electron microscope (TEM) (JEOL Ltd., Akishima, Tokyo, Japan). One drop of the optimized dispersion was applied to a carbon-covered grid, distributed in water, and left to dry. Then, 1% phosphotungstic acid was used to inspect and dry the optimized Ana-SPLs (negative staining) [38].

***Fourier transform infrared spectroscopy (FTIR) compatibility study*:**

FTIR spectroscopy (Alpha II, Bruker, Germany) was used to test the drug's compatibility with various nanoparticle excipients. For comparison, the FTIR spectrum of the pure Ana was investigated, along with the FTIR spectrum for the physical mixtures at a 1:1 (w/w) ratio and the optimal formula. The FTIR spectra were recorded in the range of 4000 and 400 cm^{-1} [39].

Differential scanning calorimetry (DSC)

A mixture of Ana and excipient in a 1:1 (w/w) and for the optimal formula were analyzed using DSC. The DSC experiment used thermal analysis equipment (STD Q 600 V20.9 Build 20, USA). The tests were performed by putting an adequate quantity of samples (4 mg) into standard aluminium pans in a distinctive manner. There were two aluminum pans utilized: one was an empty pan used as a reference, and the other was used to analyze the sample. Before analysis, the reference pan was compressed and crimped, and the other pan was filled with the model and sealed. The temperature of the device was increased from 25–300 °C while using nitrogen gas and maintaining a steady heating rate of 10 °C/min purged with a 50 mL/min flow rate [36].

Statistical analysis

A response-surface-randomized User-Defined design (Design Expert® application (Version 11.0) optimized Ana-SPLs with appropriate physicochemical characteristics. The method uses two numerical factors: the ratio of span-to-edge activator weight (Span: EA, X1) and the sonication time (ST, X2). Another factor that was taken was the edge activator type (EA, X3), which is a category-type factor. The literature was used to guide the selection of independent variables, and our lab's preliminary testing was used to establish their ranges. The response variables were the particle size (Ps, Y1, nm) and zeta potential (Zp, Y2, mV). The values of the examined variables and the response targets are enumerated in Table. 1. Twelve suggested runs were produced. The mixture of components on individual design points is shown in Table. 2. ANOVA, or statistical analysis of variance, was used to ascertain how independent variables affected the responses at a significant level ($p < 0.05$).

Table 1. Levels of independent variables and desired response limitations for Ana-SPLs formulations using a response-surface randomized User-Defined design.

Symbol	Independent Variables	Levels			
X1:	Span: Edge activator ratio (w/w)	3	9:1	7:3	5:5
X2:	Sonication duration	2	0	5	
X3:	Edge activator type	2	Tween 80	SDC	

Table 2. Experimental runs using the response-surface randomized design and their respective responses.

RUN	X1	X2	X3	Y1	Y2
1	7: 3	5	SDC	155±2.5	-34.2±1.4
2	9: 1	5	SDC	138.1±3	-32.4±1.7
3	9 :1	0	Tween 80	139.6±3.8	-22.3±3.4
4	5:5	0	SDC	194.8±3.3	-32.54±2.5
5	5:5	5	SDC	205.6±2.1	-36.4±1.2
6	5:5	0	Tween 80	123.6±4.2	-20.01±3.1
7	9 :1	5	Tween 80	133.5±3.5	-25.7±1.1
8	7:3	5	Tween 80	120.3±1.5	-24±2.4
9	5:5	5	Tween 80	125.3±2.4	-26.7±0.6
10	7:3	0	SDC	162.1±3.7	-30.1±2.1
11	9:1	0	SDC	132.5±2.7	-28±3.4
12	7:3	0	Tween 80	130.6±4.2	-22.5±2.5

*** Results are presented as mean ± standard deviation (n = 3).**

Results and Discussion

The delivery system's size is one of the most critical factors determining medication penetration across the cellular membrane; nanoscale devices have better permeation capabilities. Also, lowering the size raises the surface area and thus may improve medication function [40]. Moreover, the size may influence reticuloendothelial system-mediated clearance, with nanoscale systems perhaps evading immune system entrapment [41]. Significant external charges afford electrostatic repelling forces, which prevent particle coalescence and agglomeration. The surface charge is well-established to represent the stability of the colloidal system. Absolut Zp values of 30 mV or more are often seen in stable systems nano-formulations [42,43].

Statistics for model fit

Data was subjected to a fitting statistical analysis to identify the polynomial model that best suited the data and represented the relationship between the factors being studied and the response. Maximum R^2 is the foundation of the suggested model. The proposed model for both responses was linear based on the fit statistics, with R2 values of 0.9098 for zeta potential and 0.9826 for particle size, respectively. Zp had R2 of 0.8751 and 0.7747, while Ps had 0.9055 and 0.9618 for both predicted and adjusted R^2. The very modest gap of less than 0.2 for both replies indicates the adequacy of the model, as shown by the satisfactory coincidence of the expected and modified R^2[44]. Furthermore, Zp and Ps had exact values of 12.6988 and 18.9373, respectively. Any number greater than 4 indicates a good signal-to-noise ratio. Thus, the linear model is ideal for navigating the experimental design space.

Analysis of diagnostics

To determine if the Ps and Zp statistics were compatible with the linear model, a diagnostic evaluation was conducted, and diagnostic plots were produced. The usual probability plans of residuals Figures. 1A and 2A show a linear pattern, which implies that the residuals have a normal distribution and do not need data processing. The measured responses, which indicate the requirement for transformation when the ratio between the greatest and lowest values is more than 10, support the lack of a need for transformation. On the other hand, if the ratio is less than 3, power transformation has no effect. The robust linearity is displayed in Figures. 1B and 2B show a remarkable association between the measured and predicted values, which compare the expected and actual responses. This outcome validates the model's validity [44]. In addition, the residual vs run plots are shown in the Figures. 1C and 2C, and the same plots are shown in the Figures. 1D and 2D. These results show randomly distributed points within the established ranges, indicating that there is no persistent error or any other variable that may affect the answers [44,45].

The diagnostic plots for Ps and Zp confirmed the adequacy of the developed model. The normal probability plot indicated normally distributed residuals, while the predicted versus actual plot demonstrated good agreement between experimental and predicted values. Additionally, the studentized and externally studentized residual plots showed random dispersion without any systematic trends or outliers, confirming homoscedasticity and experimental consistency. These findings validate the suitability of the model for predicting Ps and Zp of Ana-SPLs.

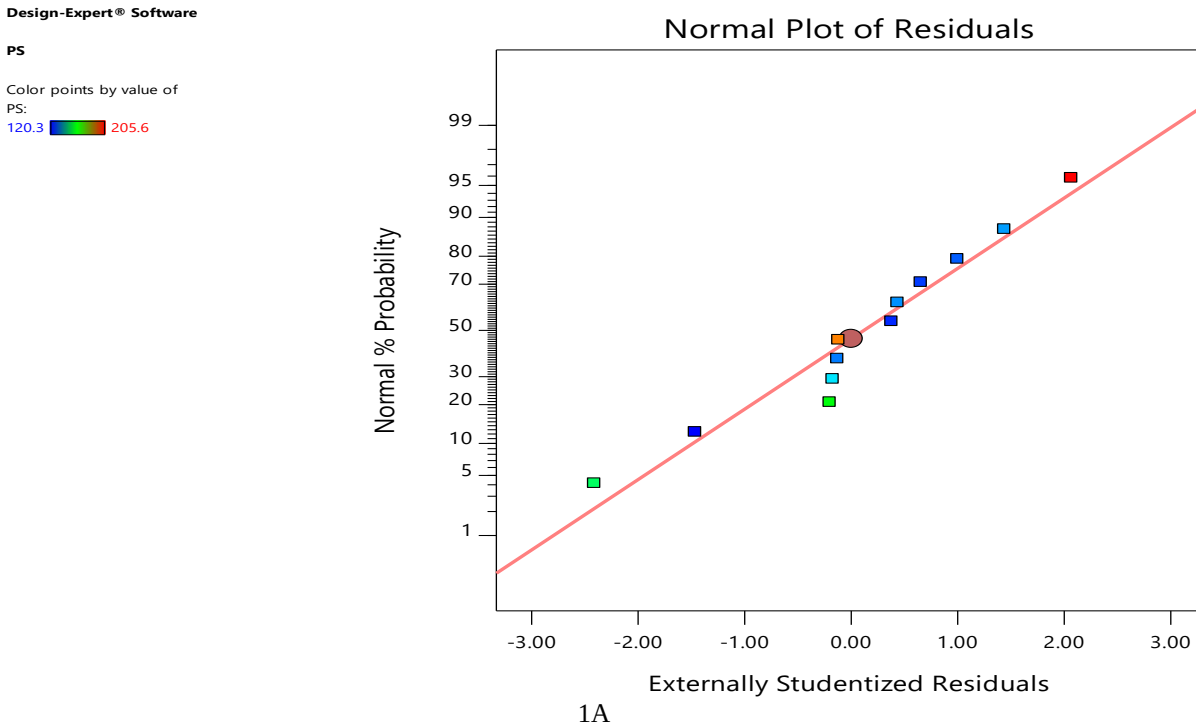

1A

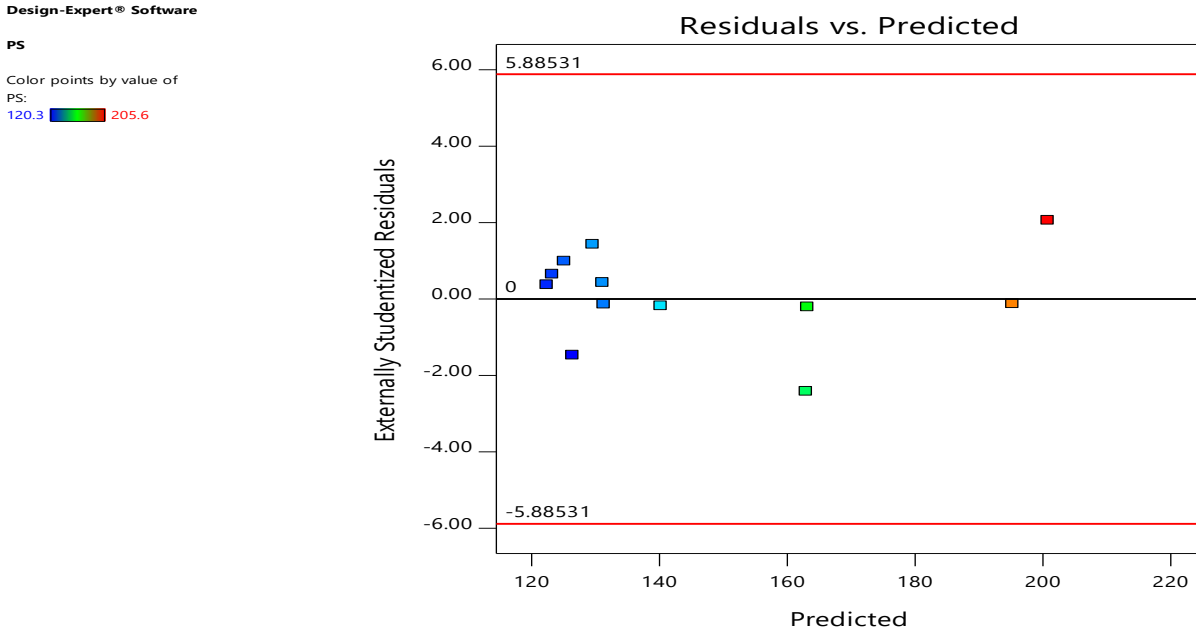
Design-Expert® Software
PS
Color points by value of
PS:
120.3
205.6
Residuals vs. Predicted
Externally Studentized Residuals
Predicted
5.88531
-5.88531
0
6.00
4.00
2.00
0.00
-2.00
-4.00
-6.00
120
140
160
180
200
220

1B

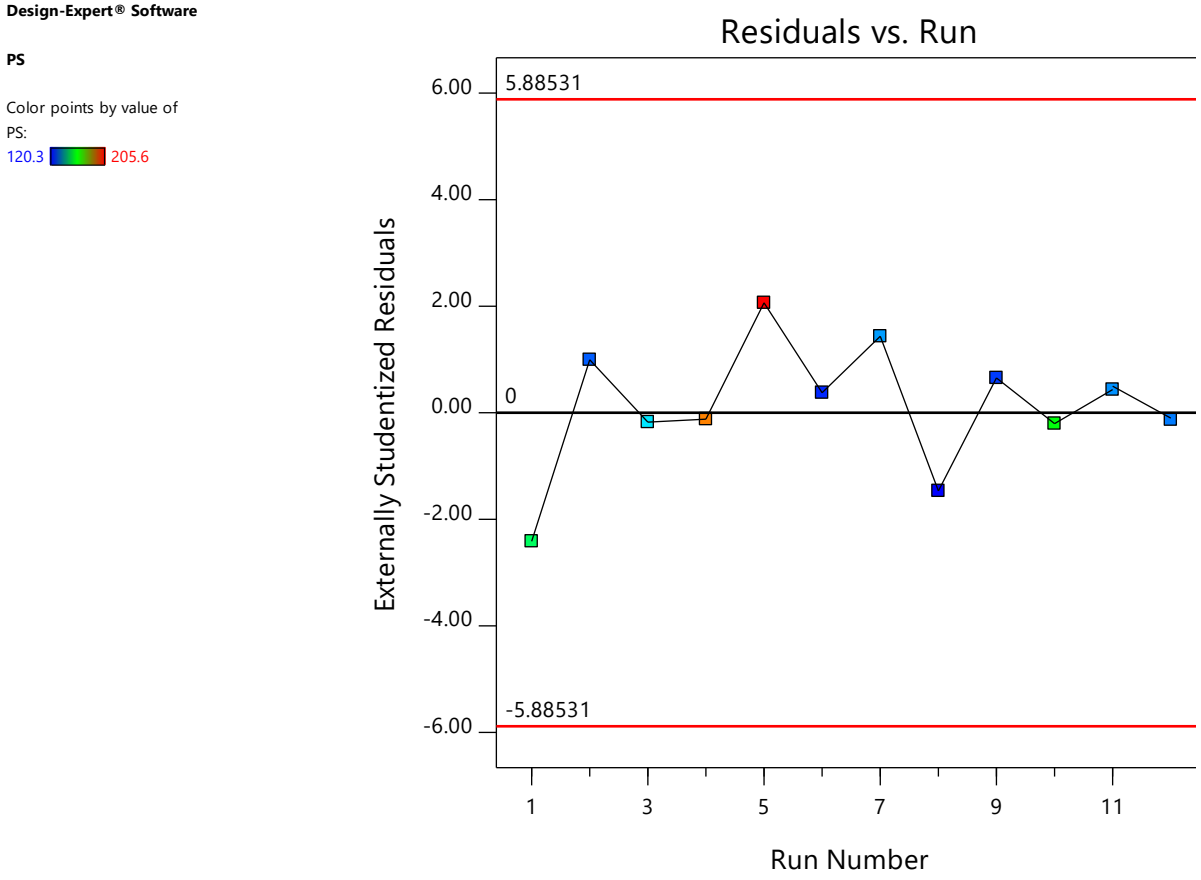
Design-Expert® Software
PS
Color points by value of
PS:
120.3
205.6
Residuals vs. Run
Externally Studentized Residuals
Run Number
5.88531
-5.88531
0
6.00
4.00
2.00
0.00
-2.00
-4.00
-6.00
1
3
5
7
9
11

1C

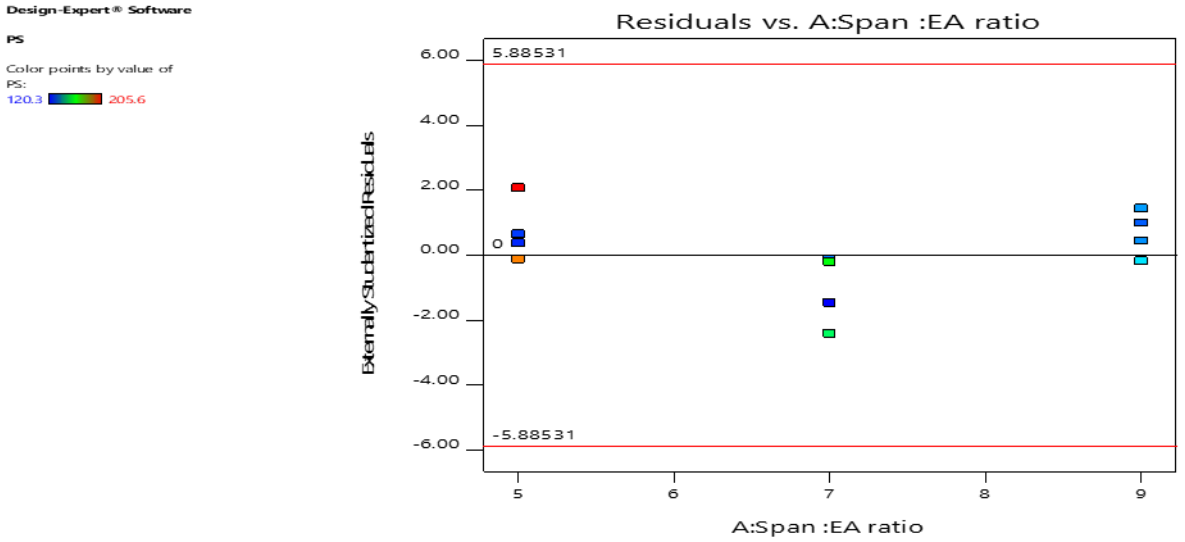

1D

Figure 1. Diagnostic plots for particle size of Ana-SPLs. (1A) Typical probability plot; (1B) predicted vs. actual values plot; (1C) studentized residuals vs. predicted values plot; (1D) externally studentized residuals vs. run number plot.

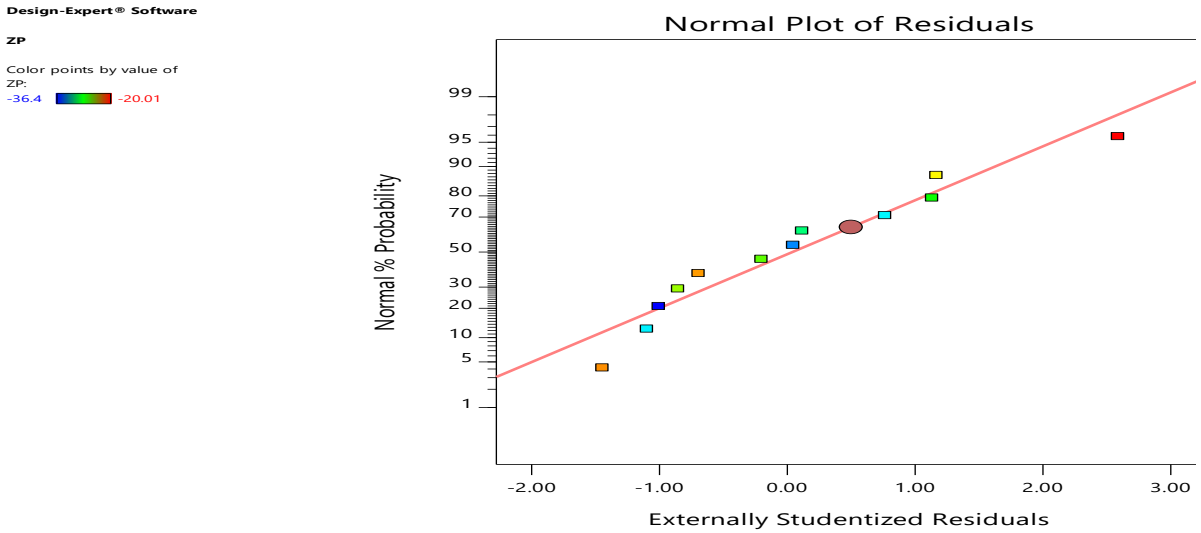

2A

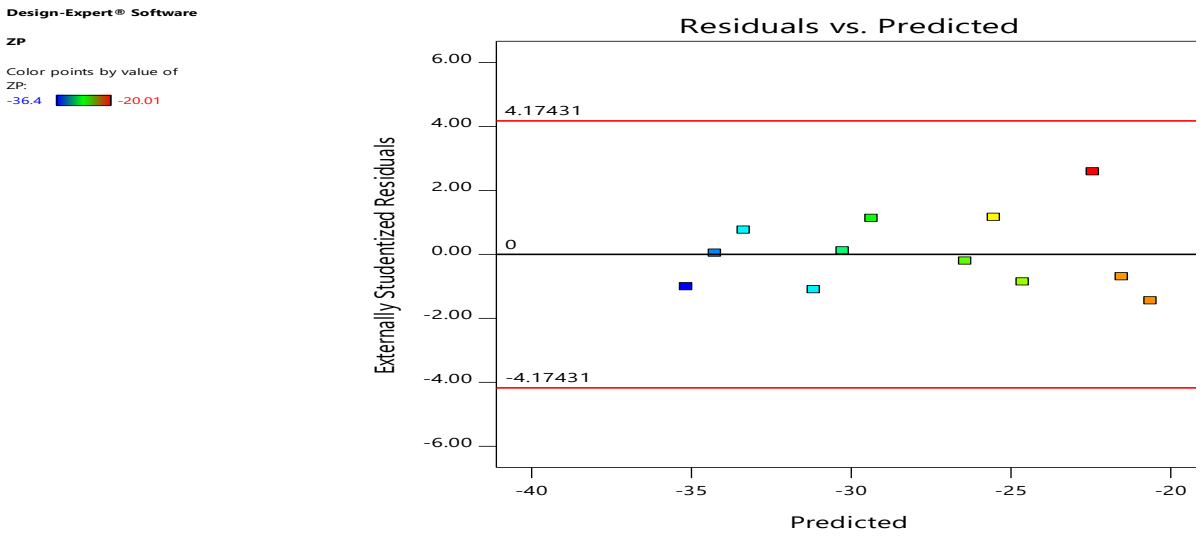

2B

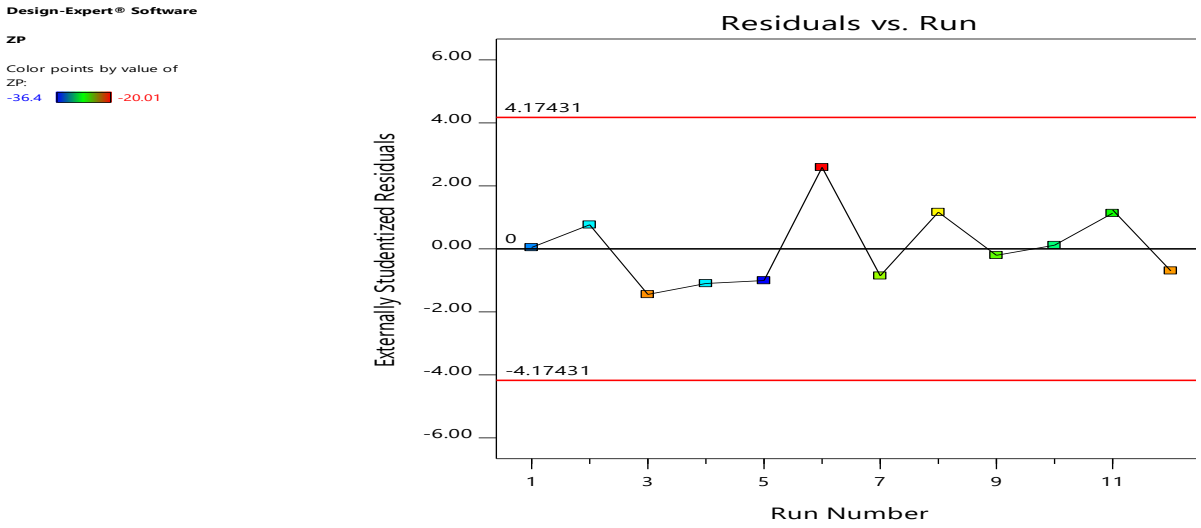

2C

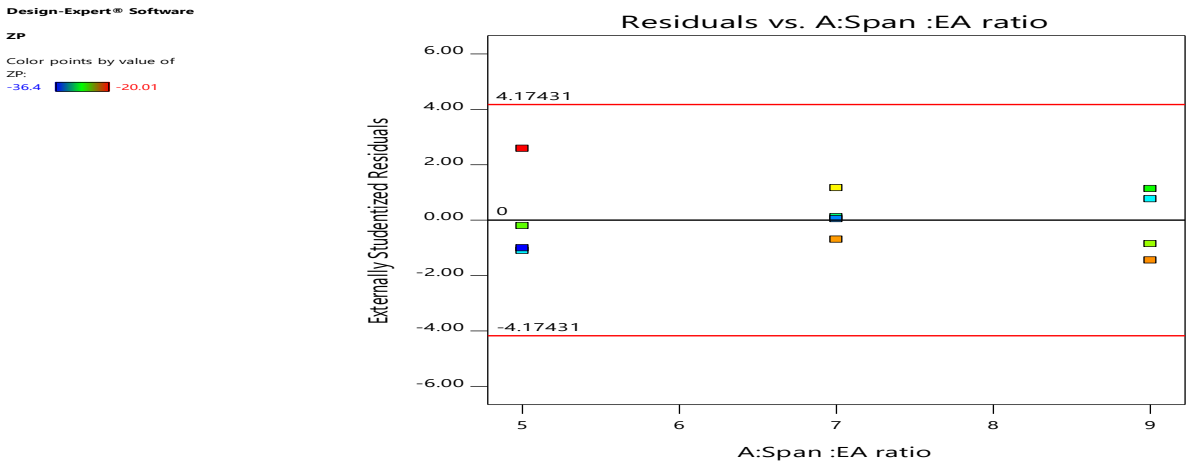

2D

Figure 2. Diagnostic plots for zeta potential of Ana-SPLs. (2A) Typical probability plot; (2B) predicted vs. actual values plot; (2C) studentized residuals vs. predicted values plot; (2D) externally studentized residuals vs. run number plot.

Statistical analysis of variables influences response (Y1)

The range Ps of the Ana-SPLs varied between (120.3±1.5 to 205.6±2.1nm) as shown in Table 2. The nanoscale range is advantageous for increasing transdermal medication delivery. The relatively low standard deviation indicates a homogeneous and uniform distribution. Analysis of variance (ANOVA) for Ps is shown in Table 3. The statistical analysis demonstrated that both the Spain: EA ratio (X1) and EA (X3) had a significant influence on the size of Ana-SPLs (P = 0.0016 and <0.0001, respectively). Figure. 3. depicts Contour plots for the specific impacts of the tested factors on the Ps.

Table 3. ANOVA of vesicle size of Ana-SPLs.

Source	Sum of squares	Degrees of freedom	Mean square	F- value	*P* – value
Model	0.0000	6	2.379	47.18	0.0003 Significant
X1: Span: EA	1.939	1	1.939	38.47	0.0016 Significant
X2:ST	1.093	1	1.093	2.17	0.2009 Nonsignificant
X3: EA type	6.342	1	6.342	125.79	<0.0001 Significant
Residual	2.521	5	5.041		
Lack of fit	5.882	3	1.961	38.89	0.0007 Significant

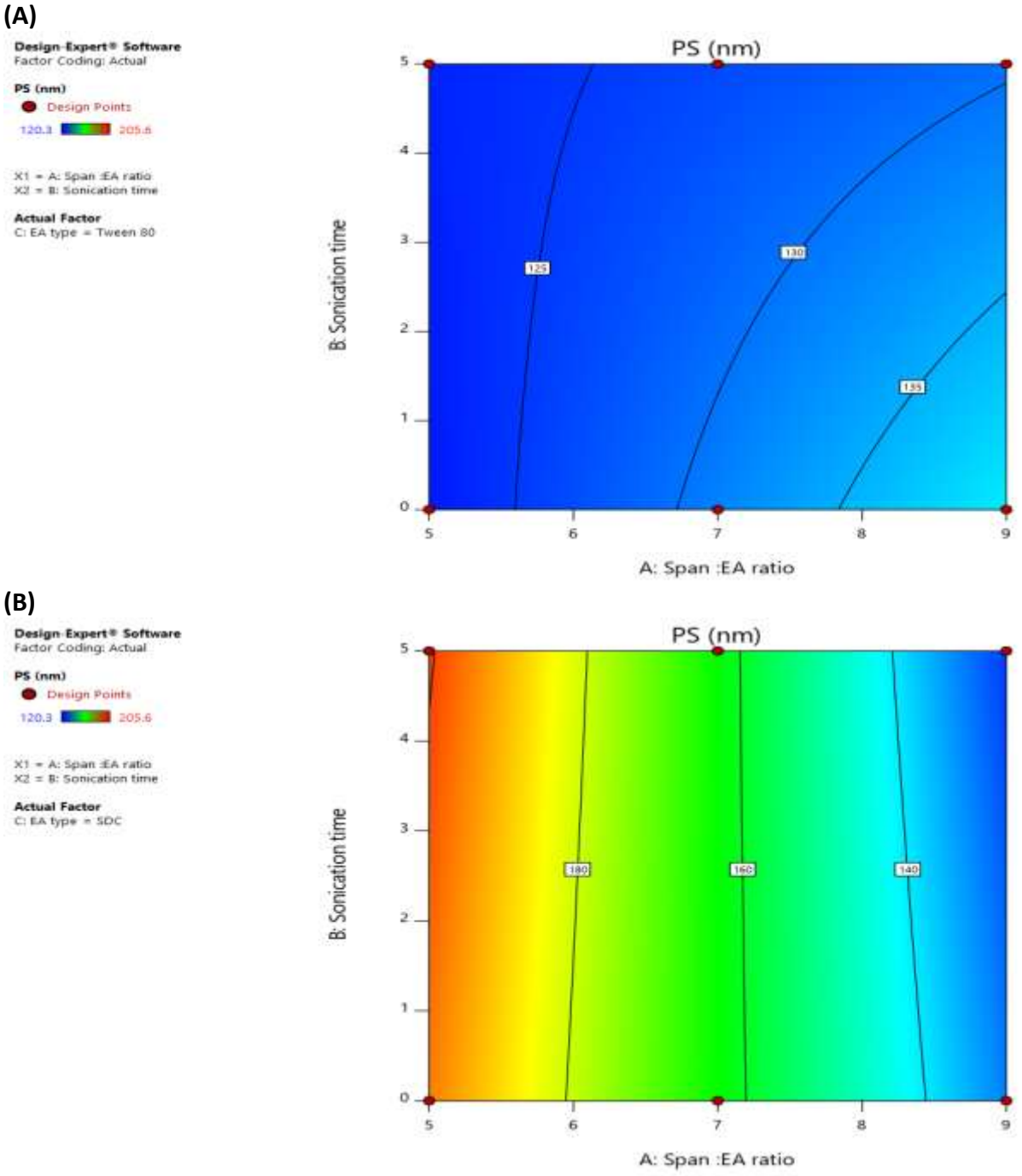

Figure 3. Contour plots illustrating the influence of Span: EA ratio and sonication time on particle size of Ana-SPLs, with EA type fixed as (A) Tween 80 and (B) SDC.

Furthermore, a study revealed that the nanocarrier's size significantly decreases as the sonication period increases. This finding is consistent with earlier investigations. Saad A *et al* [46] found a substantial negative association between ethylcellulose-based microsponges nanoparticle size and sonication duration. Badr-Eldin *et al.* [47] found a comparable negative association with simvastatin spanlastic size and sonication duration in the alternative investigation. The influence of sonication duration on size might be described by the pressure energies generated by ultrasonication waves passing through the formulation's colloidal system. Such energies might cause particle fractionation and size decrease [48]. Concerning the EA type, Ana-SPL sizes where the EA used were SDC are higher than when Tween 80 was used. This result may be due to the HLB value of the edge activators used. SDC has the maximum HLB value of (HLB = 16.7), and Tween 80 (HLB = 15). As stated earlier, the HLB value is directly linked to the SPL size. Surfactants with higher HLB values may have larger particle sizes owing to increased surface energy and water absorption [49].

Statistical Analysis of Variables' Influence on Zp (Y2)

Zeta potential (Zp), a measure of the particle surface charge, is an essential physical stability indicator that prevents aggregation formation. Significant electrostatic repulsion prevents particle clumping and stabilizing nano-sized systems with Zp values greater than ±30 mV [43,50]. The Zp charge of the prepared Ana-SPLs formula ranged from -20.01±3.1 to -36.4 ± 1.2, as Table 2. demonstrates. The partially negative groups present in the polar head of Span may be connected to the negative charge of the SPLs. A net negative charge for the generated SPLs may be shown by the orientation of such polar heads toward the external aqueous phase [51]. The linear model's applicability was confirmed by the ANOVA analysis, which generated an F-value of 26.69 ($p < 0.0002$) (Table 4.). Span: The Zp of Ana-SPLs is strongly impacted by EA (X1) ratio and EA type (X3) (p = 0.035 and <0.0001, respectively). The EA-type effect was more significant than the ratio of Span to EA, as indicated by the more significant *p*-value.

Table 4. ANOVA of zeta potential of Ana-SPLs.

Source	Sum of squares	Degrees of freedom	Mean square	F- value	*p*-value
Model	0.0005	3	0.002	26.69	0.0002 Significant
X1: Span: EA	0.0001	1	0.0001	14074	0.035 Significant
X2:ST	2.717	1	2.717	0.4316	0.5296 Nonsignificant
X3: EA type	0.0004	1	0.0004	64.89	<0.0001 Significant
Residual	0.0001	8	6.294		
Lack of fit	0.0005	3	0.0002	26.69	0.0002 Significant
Cor total	0.0006	11			

Contour plots illustrating each studied factor's unique influence on the Zp are shown in Figure. 4. Ana-SPLs formula created with SDC exhibited a higher Zp than those prepared with Tween 80 concerning the EA type. Additionally, Table 2 illustrates how the Span: EA ratio was particularly noticeable regarding SDC, as the Zp increased significantly as edge activator levels increased. There was no discernible difference in kinds or ratios among the other edge activators. This finding might be explained by the fact that SDC has a negative charge as opposed to the nonionic nature of the different surfactants [52]. As shown in previous results by Ansari, MD [53], there is no significant difference in sonication duration.

(A)

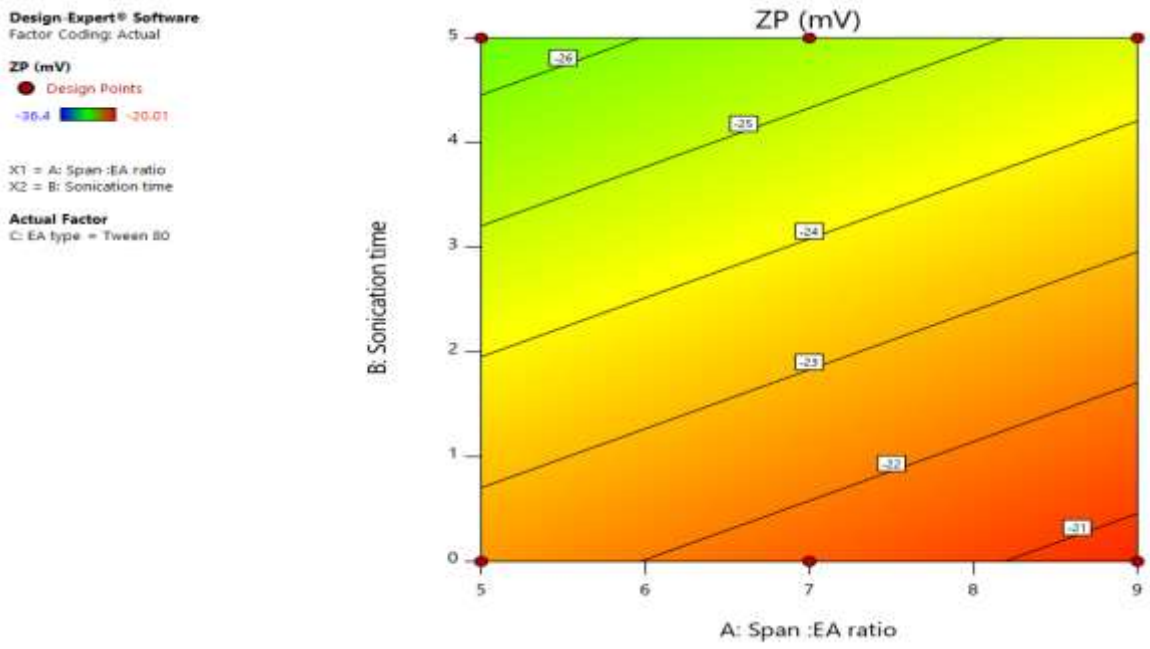

(B)

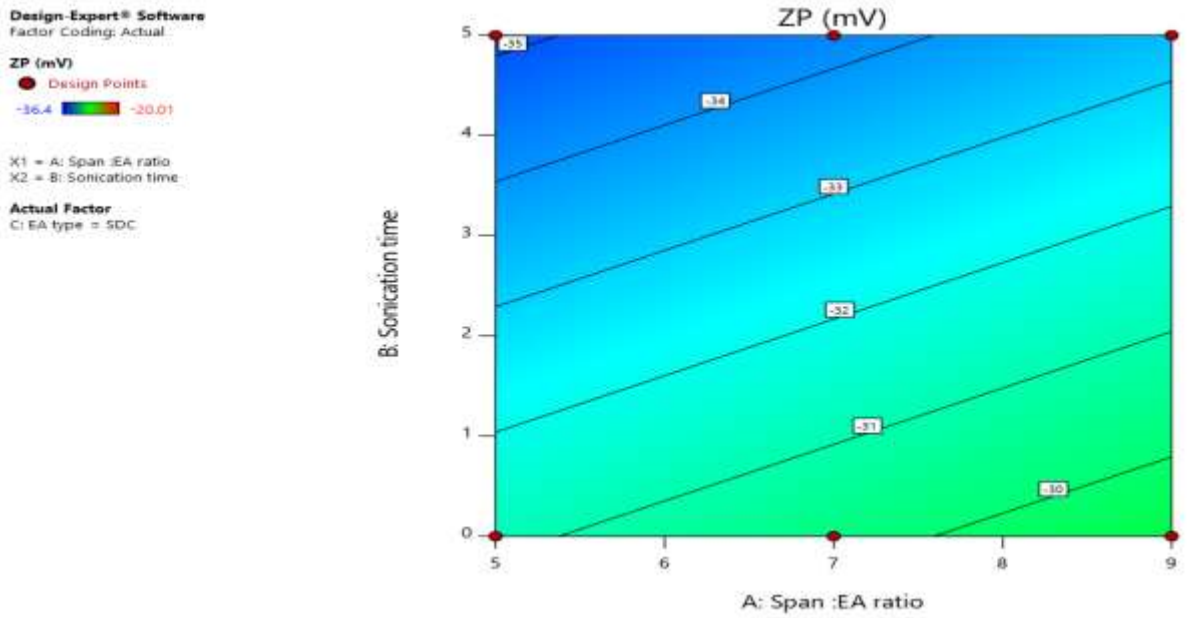

Figure 4. Contour plots illustrating the influence of Span:EA ratio and sonication time on Zp of Ana-SPLs, with EA type fixed as (A) Tween 80 and (B) SDC.

Optimization of Ana-SPLs.

Pharmaceutical optimisation primarily aims to predict the quantities of variables that will produce a formulation with the desired properties. Using the Design-Expert software, Ana-SPL's nanospanlastic formulation optimisation was achieved by numerically refining the values of several factors [(54)]. When all variables were combined, the programme predicted the values of independent variables most likely to accomplish the goals, with the highest desirability (minimise Ps and maximise Zp). Figure 5A shows the ramp graphs with optimal levels and projected responses, while Figure 5B displays the desirability values. The predicted combination of factors has an overall desirability of 0.97, which is sufficient to attain the targeted response objectives. The measured responses for size were 138.1 ± 3 nm and −32.4 ± 1.7 mV for Zp, indicating excellent penetration and stability against aggregation. The predicted and actual responses aligned well, with Ps and Zp showing low relative error percentages of 5.15% and 8.82%%, respectively. This relatively low error rate confirms the reliability of the optimisation process. According to the results, F2 achieved a higher desirability score of 0.974. Consequently, F2 was selected for further research as the potential nanospanlastic candidate deemed optimal. Span 60, a nonionic surfactant, and SDC, an EA, were combined to create the optimal formula (F2) at a weight ratio of 9:1. The ethanol injection technique was employed, with a sonication period of 5 minutes.

A

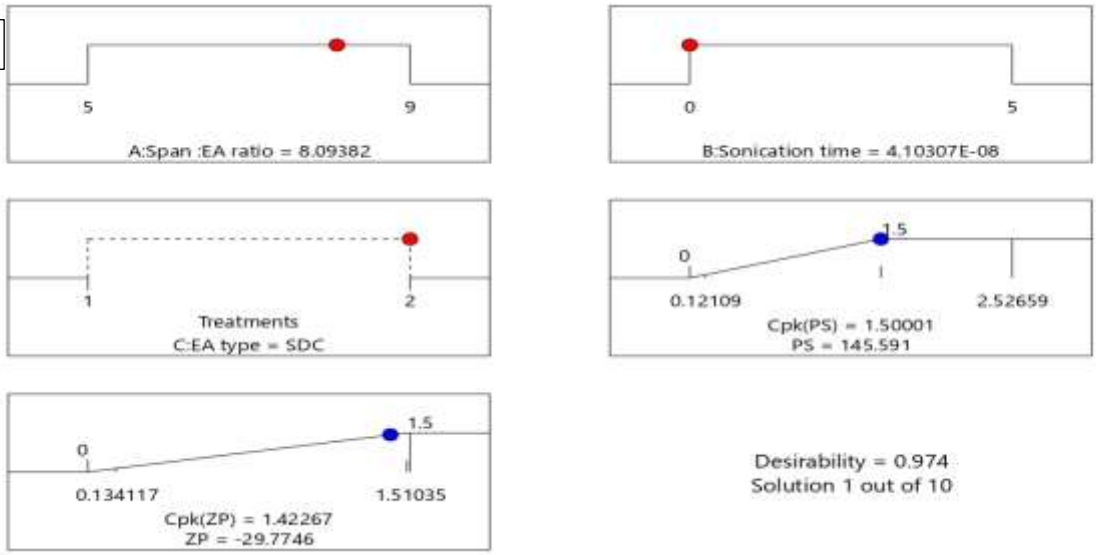

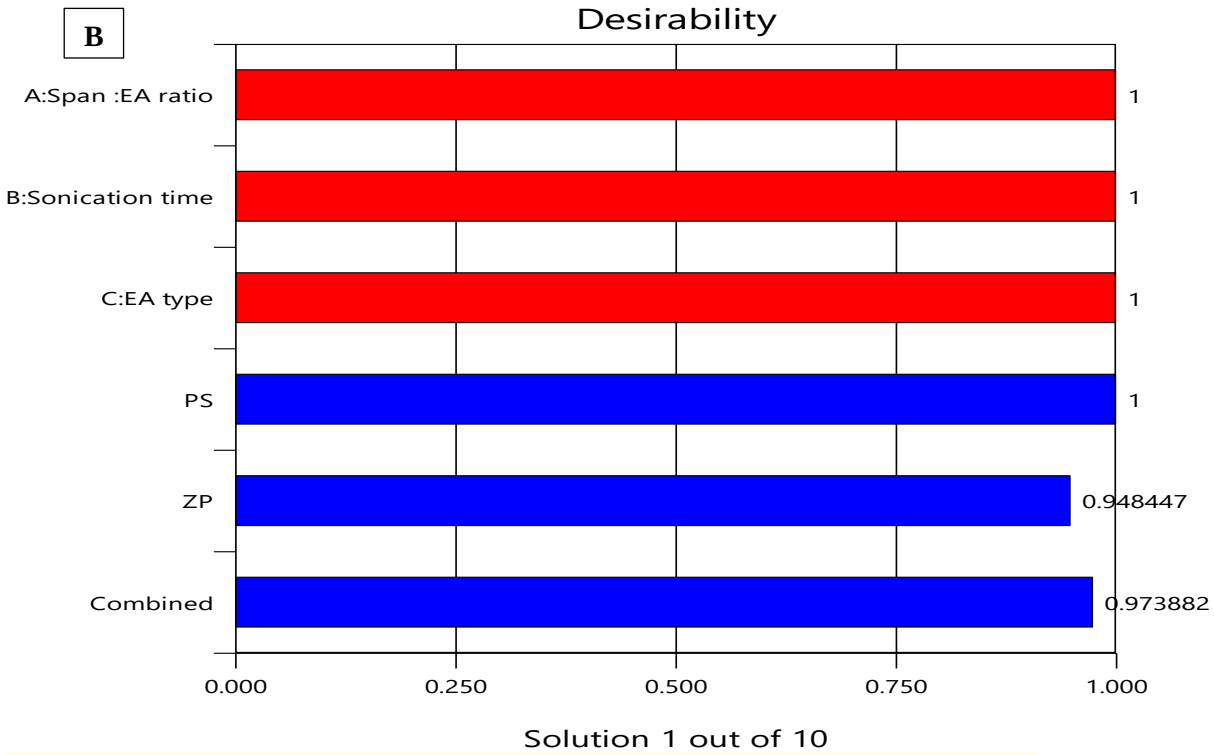

Figure 5. (A) Ramp graphs for the optimized variable levels and predicted responses of the optimized Ana-SPLs; (B) bar graph for the desirability of the optimization process.

Determination of optimal Ana-SPLs Entrapment efficiency result of an optimal formula

The EE% optimized Ana-SPLs revealed that 80.2 ± 4.3% of Ana were trapped in the ideal formula F2.

Transmission electron microscopy (TEM) analysis results

As shown in the Figure. 6, the optimized Ana-SPLs TEM image displays distinct sphere-like nanostructures (without aggregation) with diameters between 21.7 and 159 nm. The TEM application uses a strategy unlike the DLS technique to assess size, and the variance in size data may be credited to preparing the sample (drying and staining) for the TEM examination, which may disturb the size distribution [(42)].

Figure 6. TEM picture of the optimized Ana-SPLs. (F2).

The in vitro release data results

Figure. 7 displayed Ana release from plain suspension and Ana release from SPLs. According to the Research, Ana-SPLs released Ana more slowly than drug suspensions. After six hours, the percentage of Ana released from SPLs was significantly lower than that of Ana suspension ($P < 0.05$). The Span 60 has a high transition temperature (TC), which creates a more inflexible, impermeable bilayer, which might cause this. Additionally, the

extended chain length of Span 60 produced more stable vesicles with delayed drug release [55]. According to the research by Ruckmani *et al*, comparative data suggested that Ana's vesicular encapsulation regulates and maintains its release for an extended duration [56]. Consequently, this lowers the drug's dosing schedule, boosts its bioavailability, and lessens its toxicity. The Korsmeyer-Peppas model is closely fitted to the data from drug release experiments. After calculating the coefficient of correlation (R^2) values, Higuchi was determined to be the model that best fitted the release patterns of the Ana nanoparticles that had been created. Korsmeyer-Peppas slope (n) was 0.6484 for the formulation under examination, indicating anomalous transport (non-Fickian) via a mix of erosion and diffusion-controlled drug release from Ana-SPLs [57].

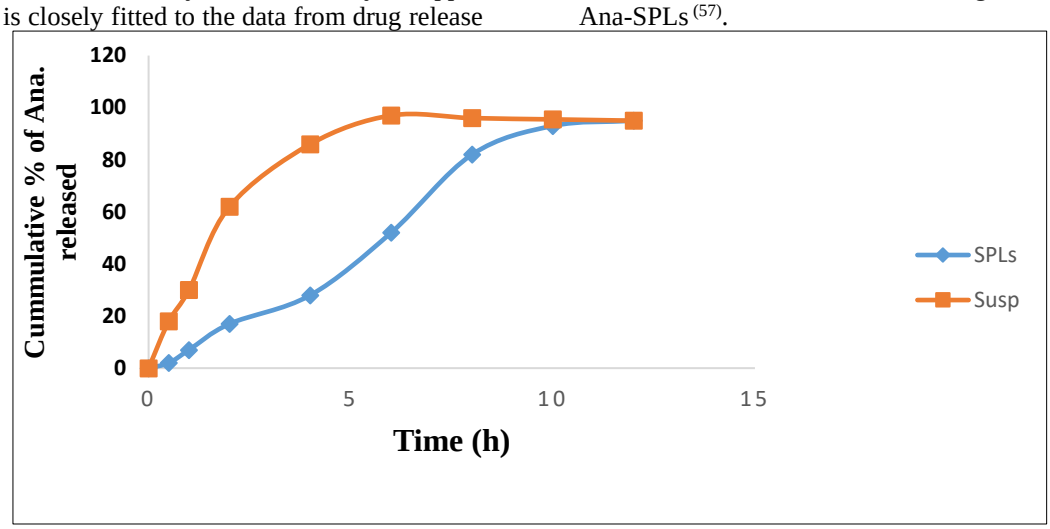

Figure 7. *In vitro* release study of optimal Ana formulation(F2).

Fourier transform infrared spectroscopy (FTIR) results

Figure. (8) FTIR spectrum of pure drug showed characteristic aromatic ring peaks at:3000–3100 cm^{-1},3100–2980 cm^{-1} representing aromatic C–H stretch of benzene, 2230–2245 cm^{-1} representing aliphatic C≡N stretch of nitrile, and 1600 to 1270 cm^{-1} representing C=N hetero aromatic. The FTIR spectrum in Figure. (9) for physical mixture and figures. (10) for optimized Ana-SPLs formula(F2), showed no overlap or presence of new peaks in the bands of the optimized Ana-SPLs formula, suggesting no meaningful significant interaction between the drug and various excipients [36].

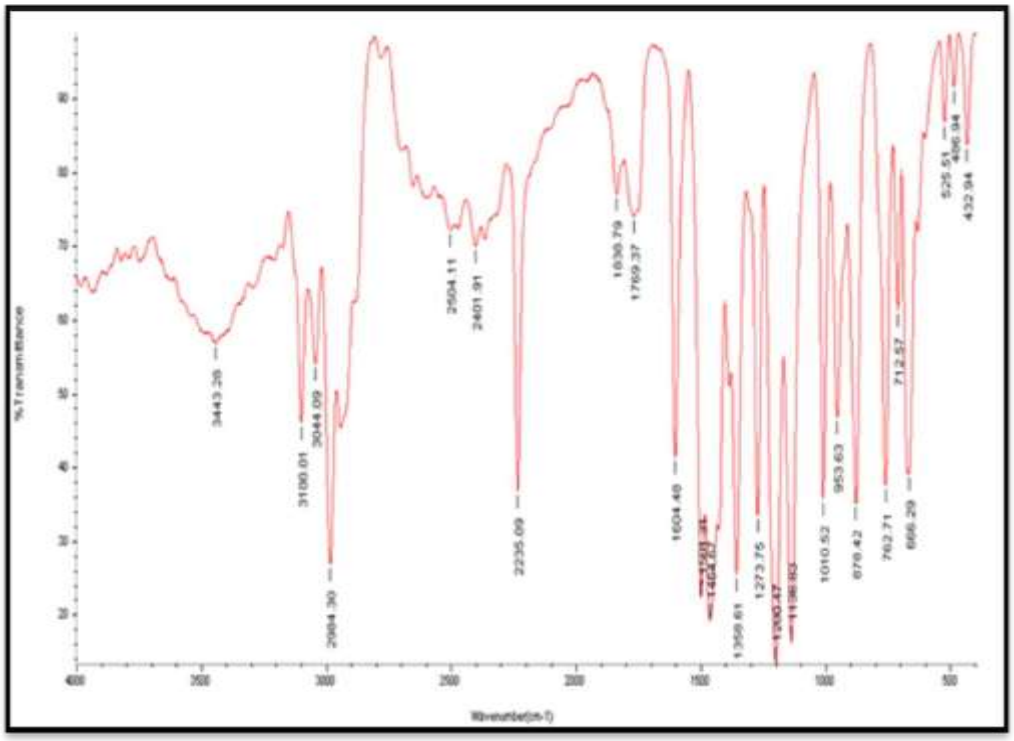

Figure 8. FTIR spectrum of Ana pure drug.

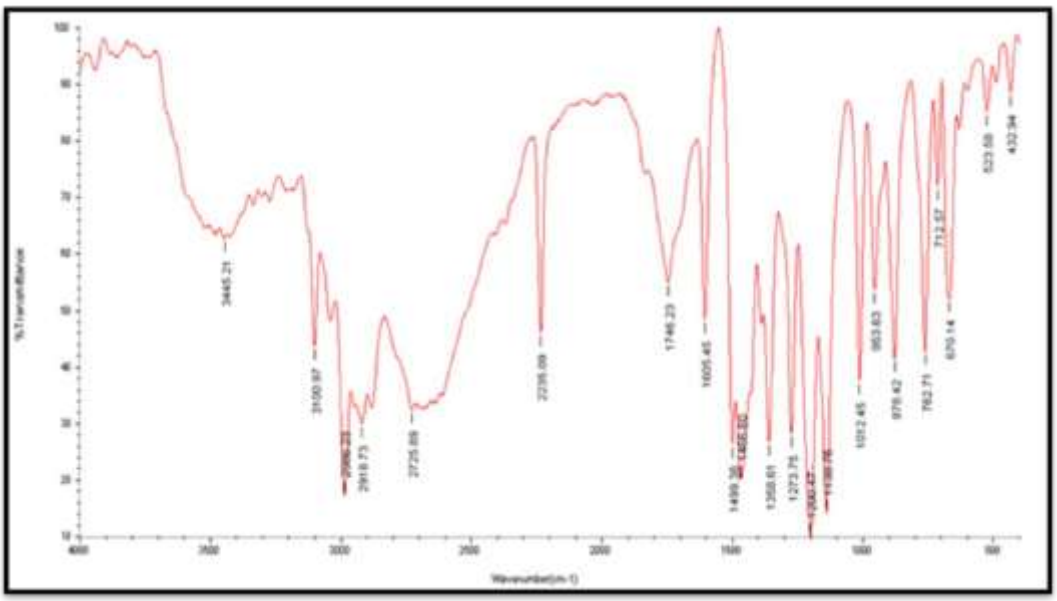

Figure 9. FTIR spectrum of Ana: polymer mixture (1: 1 w/w)

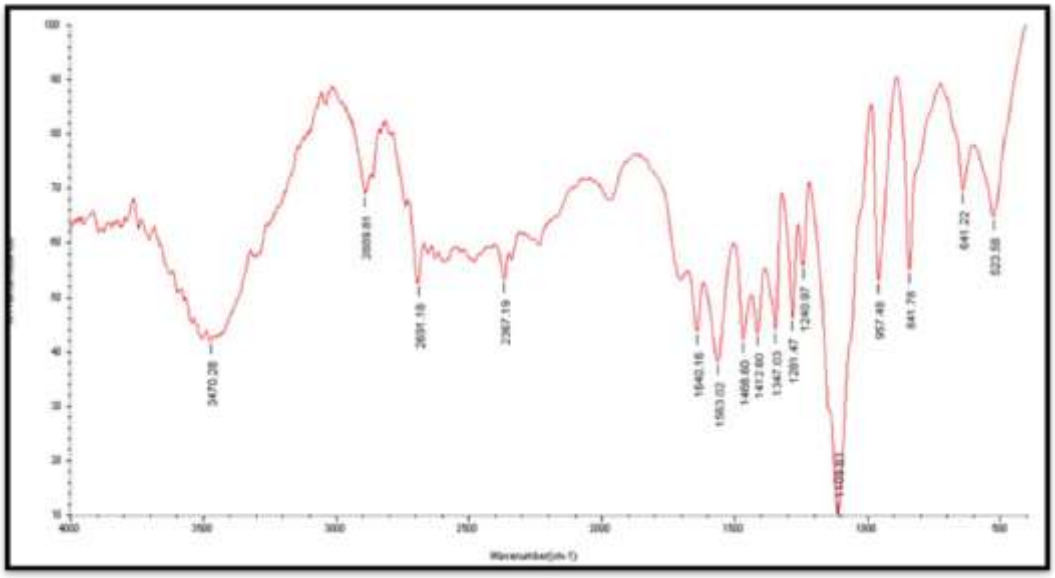

Figure10. FTIR spectrum of optimized Ana-SPLs formula(F2).

***Scanning differential calorimetry (DSC)* results**

According to the DSC thermogram, Ana exhibits a noticeable endothermic peak at its melting point of 86.52 °C, as shown in Figure. 11. This sharp endothermic peak suggests that Ana was crystallin pure powder in comparison to the standard [58]. At 54.4°C, span 60 had a distinctive endothermic peak corresponding to its transition temperature [59,60]. Figure. 12 thermograms of the physical mixtures of Ana and the excipients used to demonstrate the medication and excipient's exceptional compatibility.

Since the Ana peaks were removed, the thermogram data in Figure. 13. showed that Ana was confined inside the spanlastics vesicles. At 53°C, a new endothermic peak corresponding to the span 60's melting point also appeared. These results are reasonably consistent with those of Mazyed *et al.* [61]; he concluded that the endothermic peak of acetazolamide's total disappearance in the DSC thermogram of the transfersomes formulation could have been caused by the loading of acetazolamide in the amorphous state inside the transfersomes nanovesicles.

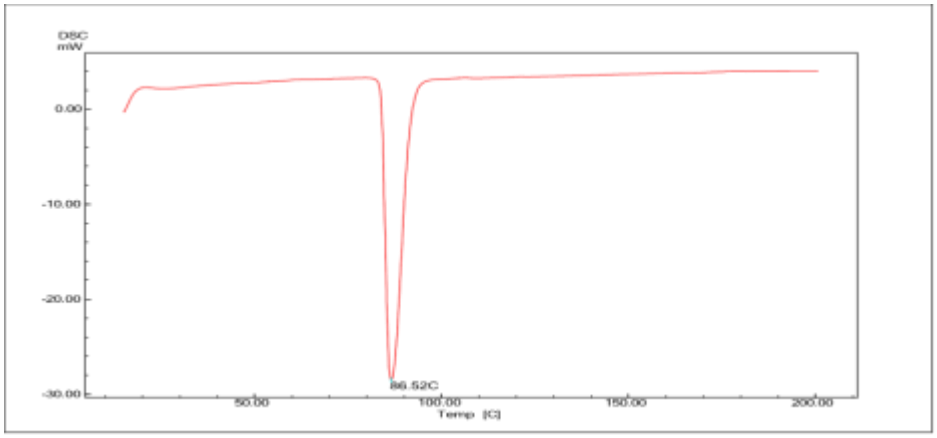

Figure 11. Thermogram of pure Anastrozole.

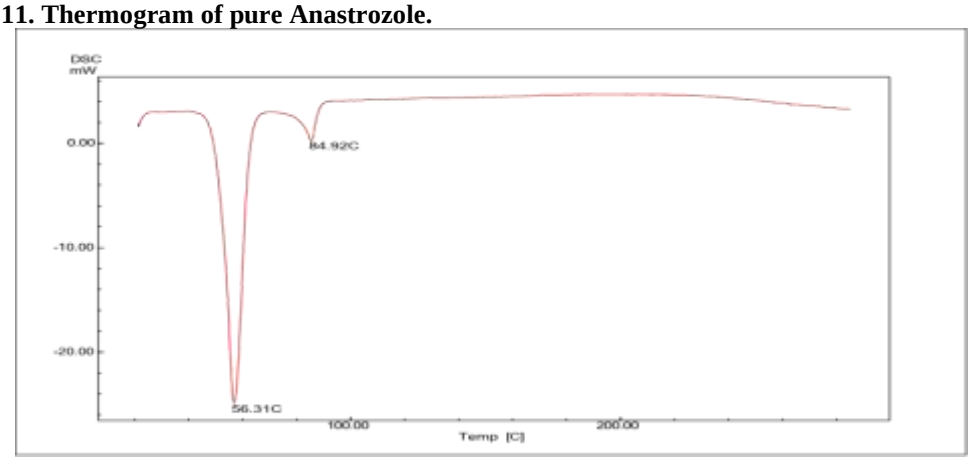

Figure 12. Thermogram of Ana with span 60 and SDC physical mixture (1: 1).

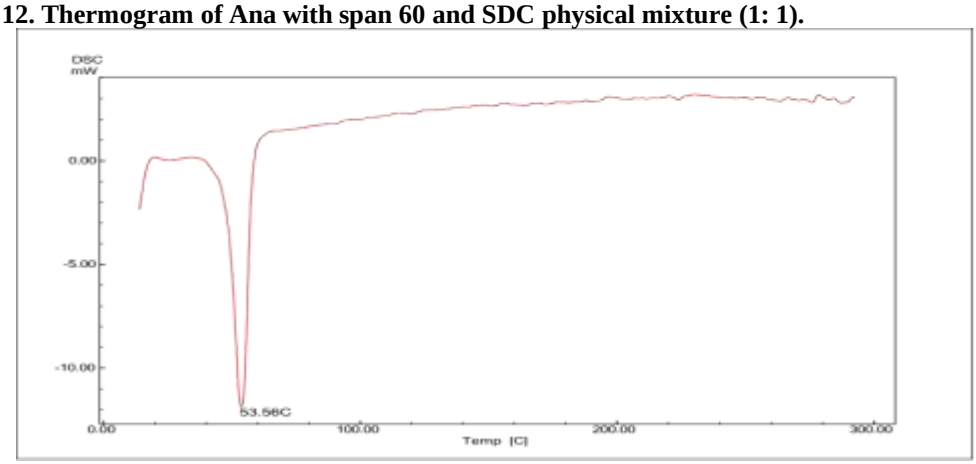

Figure 13. Thermogram of optimized Ana-SPLs formula(F2).

Conclusion

A user-defined response surface design was used to optimize nanospanlastic compositions. The findings suggested that Ana-SPLs would be a promising vesicular delivery for increasing and sustaining Ana's transdermal delivery. Transmission electron microscopes (TEM) revealed that the optimal formulation (F2) had a spherical shape with well-defined vesicles, a practical size in a nano size range of 138 nm, an acceptable zeta potential -32, and a relatively high entrapment percentage. The tests using DSC and FTIR revealed excellent encapsulation of Ana inside SPLs and the lack of interaction between anastrozole and other excipients. Using the ethanol injection technique with Span 60 and SDC as EA in the present study effectively produced promising nano-sized elastic vesicles, Ana-SPLs. The obtained data indicate that nano-spanlastics may significantly enhance Ana's permeation and release across the skin membrane.

Acknowledgement

The authors thank Baghdad University's College of Pharmacy's Department of Pharmaceutics.

Conflicts of Interest

None.

Funding

None.

Ethics Statements

No study was done on humans or animals.

Author Contribution

The authors confirm their contribution to the work. Each author evaluated the findings and approved the manuscript's final draft.

References

1. Stebbing J, Ngan S. Breast cancer (metastatic). BMJ Clinical Evidence. 2010;2010.
2. Hortobagyi GN, Buzdar AU. Anastrozole (Arimidex®), a new aromatase inhibitor for advanced breast cancer: mechanism of action and role in management. Cancer investigation. 1998 Jan 1;16(6):385-90.
3. Heer E, Harper A, Escandor N, Sung H, McCormack V, Fidler-Benaoudia MM. Global burden and trends in premenopausal and postmenopausal breast cancer: a population-based study. The Lancet Global Health. 2020 Aug 1;8(8):e1027-37.
4. Coughlin SS. Epidemiology of breast cancer in women. Breast Cancer Metastasis and Drug Resistance: Challenges and Progress. 2019:9-29.
5. Kunstič TT, Debeljak N, Tacer KF. Heterogeneity in hormone-dependent breast cancer and therapy: Steroid hormones, HER2, melanoma antigens, and cannabinoid receptors. Advances in Cancer Biology-Metastasis. 2023 Jul 1; 7:100086.
6. Horwitz KB, Sartorius CA. Ninety years of progesterone: progesterone and progesterone receptors in breast cancer: past, present, future. Journal of Molecular Endocrinology. 2020 Jul 1;65(1):T49-63.
7. Allison KH, Hammond ME, Dowsett M, McKernin SE, Carey LA, Fitzgibbons PL, Hayes DF, Lakhani SR, Chavez-MacGregor M, Perlmutter J, Perou CM. Estrogen and progesterone receptor testing in breast cancer: American Society of Clinical Oncology/College of American Pathologists guideline update. Archives of pathology & laboratory medicine. 2020 May 1;144(5):545-63.
8. Refaat B, Aslam A, Idris S, Almalki AH, Alkhaldi MY, Asiri HA, Almaimani RA, Mujalli A, Minshawi F, Alamri SA, AlHussain MI. Profiling estrogen, progesterone, and androgen receptors in colorectal cancer in relation to gender, menopausal status, clinical stage, and tumour sidedness. Frontiers in Endocrinology. 2023 May 3; 14:1187259.
9. Iacopetta D, Ceramella J, Baldino N, Sinicropi MS, Catalano A. Targeting breast cancer: An overlook on current strategies. International Journal of Molecular Sciences. 2023 Feb 11;24(4):3643.
10. Navaei NM, Navaei NM. Unlocking the potential of aromatase inhibitors: recent advances in drug design, synthesis, docking activity, and in vitro bioactivity evaluations. Synthesis and Sintering. 2023 Dec 2;3(4):234-40.
11. Emond R, Griffiths JI, Grolmusz VK, Nath A, Chen J, Medina EF, Sousa RS, Synold T, Adler FR, Bild AH. Cell facilitation promotes growth and survival under drug pressure in breast cancer. Nature Communications. 2023 Jun 29;14(1):3851.
12. Kasar RR, Ahir KN. Current and emerging biomarkers in breast cancer: A review. World Journal of Biology Pharmacy and Health Sciences. 2024;17(3):001-25.
13. In: Carrell DT, Pastuszak AW, Hotaling JM, editors. Men's Reproductive and Sexual Health Throughout the Lifespan: An Integrated Approach to Fertility, Sexual Function, and Vitality. Cambridge: Cambridge University Press; 2023. p. 264–8
14. Najm A, Niculescu AG, Grumezescu AM, Beuran M. Emerging Therapeutic Strategies in Sarcopenia: An Updated Review on Pathogenesis and Treatment Advances. International Journal of Molecular Sciences. 2024 Apr 12;25(8):4300.
15. Goldhirsch A, Wood WC, Gelber RD, Coates AS, Thurlimann B, Senn HJ. Meeting highlights: updated international expert consensus on the primary therapy of early breast cancer. Journal of Clinical Oncology. 2003 Sep 1;21(17):3357-65.
16. Huppert LA, Gumusay O, Idossa D, Rugo HS. Systemic therapy for hormone receptor-positive/human epidermal growth factor receptor 2-negative early stage and metastatic breast cancer. CA: A Cancer Journal for Clinicians. 2023 Sep;73(5):480-515.
17. Seary H, Barakat EH, Raslan MA, Samy AM. Development, characterization, and optimization of repaglinide loaded spanlastics along with investigation of drug solubility in various media. Universal Journal of Pharmaceutical Research. 2024 Nov 15.
18. Ansari MD, Saifi Z, Pandit J, Khan I, Solanki P, Sultana Y, Aqil M. Spanlastics a novel nanovesicular carrier: Its potential application and emerging trends in therapeutic delivery. AAPS PharmSciTech. 2022 Apr 11;23(4):112.
19. Gad S, Hanna P, Ibrahim H, Mortagi Y. Surfactants' Role in Nanovesicles Drug Delivery System. Records of Pharmaceutical and Biomedical Sciences. 2023 Jan 1;7(3):140-9.
20. Ali AA, Hassan AH, Eissa EM, Aboud HM. Response surface optimization of ultra-elastic nanovesicles loaded with deflazacort tailored for transdermal delivery: Accentuated bioavailability and anti-inflammatory efficacy.

International Journal of Nanomedicine. 2021 Jan 25:591-607.

21. Saini H, Rapolu Y, Razdan K, Nirmala, Sinha VR. Spanlastics: a novel elastic drug delivery system with potential applications via multifarious routes of administration. Journal of Drug Targeting. 2023 Nov 26;31(10):999-1012.

22. Muzammil S, Mazhar A, Yeni DK, Andleeb R, Ashraf A, Shehzad MI, Zafar N, Mazhar M. Nanospanlastic as a promising nanovesicle for drug delivery 2022 Jan 1 (pp. 337-352). Academic Press.

23. Ansari MD, Saifi Z, Pandit J, Khan I, Solanki P, Sultana Y, Aqil M. Spanlastics a novel nano vesicular carrier: its potential application and emerging trends in therapeutic delivery. AAPS PharmSciTech. 2022 Apr 11;23(4):112.

24. Al-Mahallawi AM, Khowessah OM, Shoukri RA. Enhanced non-invasive trans-tympanic delivery of ciprofloxacin through encapsulation into nano-spanlastic vesicles: Fabrication, in-vitro characterization, and comparative ex-vivo permeation studies. International journal of pharmaceutics. 2017 Apr 30;522(1-2):157-64.

25. Abdelbari MA, El-Mancy SS, Elshafeey AH, Abdelbary AA. Implementing spanlastics for improving the ocular delivery of clotrimazole: in vitro characterization, ex vivo permeability, microbiological assessment and in vivo safety study. International Journal of Nanomedicine. 2021 Sep 10:6249-61.

26. Elsherif NI, Shamma RN, Abdelbary G. Terbinafine hydrochloride trans-ungual delivery via nano vesicular systems: in vitro characterization and ex vivo evaluation. AAPS PharmsciTech. 2017 Feb; 18:551-62.

27. Placha D, Jampilek J. Chronic inflammatory diseases, anti-inflammatory agents and their delivery nanosystems. Pharmaceutics. 2021 Jan 6;13(1):64.

28. Mazyed EA, Helal DA, Elkhoudary MM, Abd Elhameed AG, Yasser M. Formulation and optimization of nanospanlastics for improving the bioavailability of green tea epigallocatechin gallate. Pharmaceuticals. 2021 Jan 15;14(1):68.

29. Fahmy AM, El-Setouhy DA, Habib BA, Tayel SA. Enhancement of transdermal delivery of haloperidol via spanlastic dispersions: entrapment efficiency vs particle size. AAPS PharmsciTech. 2019 Apr; 20:1-3.

30. Ibrahim SS, Abd-Allah H. Spanlastic nanovesicles for enhanced ocular delivery of vanillic acid: design, in vitro characterization, and in vivo anti-inflammatory evaluation. International Journal of Pharmaceutics. 2022 Sep 25; 625:122068.

31. Badria F, Mazyed E. Formulation of nanospanlastics as a promising approach for improving the topical delivery of a natural leukotriene inhibitor (3- acetyl-11-keto-β-boswellic acid): statistical optimization, in vitro characterization, and ex vivo permeation study. Drug design, development and therapy. 2020 Sep 15:3697-721.

32. Ibrahim MM, Basalious EB, El-Nabarawi MA, Makhlouf AI, Sayyed ME, Ibrahim IT. Nose to brain delivery of mirtazapine via lipid nanocapsules: Preparation, statistical optimization, radiolabeling, in vivo biodistribution and pharmacokinetic study. Drug Delivery and Translational Research. 2024 Feb 20:1-9.

33. Mekkawy AI, Eleraky NE, Soliman GM, Elnaggar MG, Elnaggar MG. Combinatorial therapy of letrozole-and quercetin-loaded spanlastics for enhanced cytotoxicity against MCF-7 breast cancer cells. Pharmaceutics. 2022 Aug 18;14(8):1727.

34. Zaki RM, Ibrahim MA, Alshora DH, El Ela AE. Formulation and evaluation of transdermal gel containing tacrolimus-loaded spanlastics: in vitro, ex vivo and in vivo studies. Polymers. 2022 Apr 9;14(8):1528.

35. Drais HK. Transdermal Delivery of Lornoxicam Hybrid Nanogel: Design, Preparation, Characterization, and In-Vitro Diffusion Evaluation. Iraqi Journal of Industrial Research. 2023 Oct 20;10(2):98-104.

36. Hashim AA, Rajab NA. Anastrozole loaded nanostructured lipid carriers: preparation and evaluation. Iraqi Journal of Pharmaceutical Sciences. 2021 Dec 11;30(2):185-95.

37. Radhi A, Ali WK, Al-Saedi F. Preparation and in vitro evaluation of synthetic high-density lipoproteins as parenteral drug delivery system for tamoxifen citrate. Iraqi Journal of Pharmaceutical Sciences. 2023 Dec 30;32(3):105-17.

38. Albassam NY, Kassab HJ. Diacerein loaded novasome for transdermal delivery: Preparation, in-vitro characterization and factors affecting formulation. Iraqi Journal of Pharmaceutical Sciences. 2023 Nov 3;32(Suppl.):214-24.

39. Abdullah TM, Khalid KA. Topical Propranolol Hydrochloride Nanoemulsion: A Promising Approach Drug Delivery for Infantile Hemangiomas. Iraqi Journal of Pharmaceutical Sciences. 2023 Nov 4;32(Suppl.):300-15.

40. Salih OS, Al-Akkam EJ. Preparation, in-vitro, and ex-vivo evaluation of ondansetron-loaded invasomes for transdermal delivery. IJPS. 2023 Dec 30;32(3):71–84. https://doi.org/10. 31351/ vol32iss3pp71-84

41. Pereira-Silva M, Jarak I, Alvarez-Lorenzo C, Concheiro A, Santos AC, Veiga F, Figueiras A. Micelleplexes as nucleic acid delivery systems for cancer-targeted therapies. Journal of controlled release. 2020 Jul 10; 323:442-62.

42. Sultan MH, Moni SS, Madkhali OA, Bakkari MA, Alshahrani S, Alqahtani SS, Alhakamy NA,

Mohan S, Ghazwani M, Bukhary HA, Almoshari Y. Characterization of cisplatin-loaded chitosan nanoparticles and rituximab-linked surfaces as target-specific injectable nano-formulations for combating cancer. Scientific reports. 2022 Jan 10;12(1):468.

43. Abbas H, El-Feky YA, Al-Sawahli MM, El-Deeb NM, El-Nassan HB, Zewail M. Development and optimization of curcumin analogue nano-bilosomes using 21.31 full factorial design for anti-tumour profiles improvement in human hepatocellular carcinoma: In-vitro evaluation, in-vivo safety assay. Drug Delivery. 2022 Dec 31;29(1):714-27.

44. Haroon H.B., Mukherjee D., Anbu J., Teja B.V. Thiolated Chitosan-Centella Asiatica Nanocomposite: A Potential Brain Targeting Strategy Through Nasal Route. AAPS PharmSciTech. 2021; 22:251.

45. Nguyen T.T.L., Maeng H.J. Pharmacokinetics and Pharmacodynamics of Intranasal Solid Lipid Nanoparticles and Nanostructured Lipid Carriers for Nose-to-Brain Delivery . Pharmaceutics . 2022 ; 14:572. doi 10. 3390 / pharmaceutics 14030572.

46. Saad A, Sabri L. Study the Variables Affecting Formulation of Ethylcellulose-based Microsponges Loaded with Clobetasol. Iraqi Journal of Pharmaceutical Sciences. 2023 Nov 3;32(Suppl.):225-34.

47. Badr-Eldin SM, Aldawsari HM, Alhakamy NA, Fahmy UA, Ahmed OA, Neamatallah T, Tima S, Almaghrabi RH, Alkudsi FM, Alamoudi AA, Alzahrani AA. Merging experimental design and nanotechnology for developing optimized simvastatin spanlastics: A promising combined strategy for augmenting the suppression of various human cancer cells. Pharmaceutics. 2022 May 9;14(5):1024.

48. Alhagiesa AW, Ghareeb MM. The Formulation and Characterization of Nimodipine Nanoparticles to enhance solubility and dissolution rate. Iraqi Journal of Pharmaceutical Sciences. 2021 Dec 11;30(2):143-52.

49. Nowroozi F, Almasi A, Javidi J, Haeri A, Dadashzadeh S. Effect of surfactant type, cholesterol content and various downsizing methods on the particle size of niosomes. Iranian journal of pharmaceutical Research. 2018;17(Suppl2):1.

50. Nourzadeh Z, Anarjan N, Ebrahimzadeh Rajaei G, Jafarizadeh-Malmiri H. Preparation and characterization of vitamin D microemulsions using two-component surface-active stabilizer system. Zeitschrift für Physikalische Chemie. 2022 Feb 23;236(2):257-74.

51. Abdelrahman F.E., Elsayed I., Gad M.K., Elshafeey A.H., Mohamed M.I. Response Surface Optimization, Ex Vivo and In Vivo Investigation of Nasal Spanlastics for Bioavailability Enhancement and Brain Targeting of Risperidone. 2017; 530:1–11.

52. Alaaeldin E, Mostafa M, Mansour HF, Soliman GM. Spanlastics as an efficient delivery system for enhancing thymoquinone anticancer efficacy: Fabrication and cytotoxic studies against breast cancer cell lines. Journal of Drug Delivery Science and Technology. 2021 Oct 1; 65:102725.

53. Ansari MD, Solanki P, Pandit J, Jahan RN, Aqil M, Sultana Y. Fabrication and optimization of raloxifene loaded spanlastics vesicle for transdermal delivery. Journal of Drug Delivery Science and Technology. 2022 Feb 1; 68:103102.

54. Basalious EB, Shawky N, Badr-Eldin SM. SNEDDS containing bioenhancers for improvement of dissolution and oral absorption of lacidipine. I: development and optimization. Int J Pharm. 2010;391 (1–2):203–211.

55. Saini H, Rapolu Y, Razdan K, Nirmala, Sinha VR. Spanlastics: a novel elastic drug delivery system with potential applications via multifarious routes of administration. Journal of Drug Targeting. 2023 Nov 26;31(10):999-1012.

56. Ruckmani K, Jayakar B, Ghosal SK. Nonionic surfactant vesicles (niosomes) of cytarabine hydrochloride for effective treatment of leukaemias: encapsulation, storage, and in vitro release. Drug Dev Ind Pharm. 2000; 26(2):217–222.

57. Souto EB, Fangueiro JF, Fernandes AR, Cano A, Sanchez-Lopez E, Garcia ML, Severino P, Paganelli MO, Chaud MV, Silva AM. Physicochemical and biopharmaceutical aspects influencing skin permeation and role of SLN and NLC for skin drug delivery. Heliyon. 2022 Feb 11.

58. Regenthal R, Voskanian M, Baumann F, Teichert J, Brätter C, Aigner A, Abraham G. Pharmacokinetic evaluation of a transdermal anastrozole-in-adhesive formulation. Drug Design, Development and Therapy. 2018 Nov 1:3653-64.

59. Salih O, Muhammed E. Preparation, evaluation, and histopathological studies of ondansetron-loaded invasomes transdermal gel. J Res Pharm. 2024;28(1)(28(1)):289–303.

60. Jaafer H, Al-Kinani KK. Formulation and Evaluation of Idebenone Microemulsion as a Potential Approach for the Transmucosal Drug Delivery Systems. Iraqi Journal of Pharmaceutical Sciences. 2024 Mar 26;33(1):79-88.

61. Mazyed EA, Abdelaziz AE. Fabrication of transgelosomes for enhancing the ocular delivery of acetazolamide: statistical optimization, in vitro characterization, and in vivo study. Pharmaceutics. 2020;12(5):465.

التصييغ والتحسين الاحصائي والتقييم المختبري للأناستروزول النانوسبانلاستك عبر الجلد

ليلى عبدالحسين علوان[١] و شيماء نزار عبدالحميد[٢]

[١] دائرة صحة ديالى، وزارة الصحة، بغداد، العراق

[٢] قسم الصيدلانيات، كلية الصيدلة، جامعة بغداد، بغداد، العراق

الخلاصة

في النساء بعد انقطاع الطمث، يقلل عقار أناستروزول من مستويات هرمون الاستروجين، مما قد يمنع تطور بعض سرطانات الثدي التي تحتاج إلى زيادة هرمون الاستروجين في الجسم. يعاني أناستروزول من تأثير المرور الاول ومحدودية الذوبان المائي، ومشاكل في الجهاز الهضمي. بالإضافة إلى ذلك، فإن تحسين نفاذية الجلد، والتحكم في إطلاق الأدوية، وحماية الجزيئات الحساسة من التدهور ليست سوى عدد قليل من استخدامات الجسيمات النانوية التي تكتسب شعبية.السبانلاستك عبارة عن حويصلات نانوية مرنة وقابلة للتغيير تعتمد على المواد الخافضة للتوتر السطحي. وهي تشتمل على منشط الحافة ومادة خافضة للتوتر السطحي غير أيونية. في هذه الدراسة، تم إنشاء مادة الأناستروزول النانوية لتحسين امتثال المريض والتحكم في تحرير الأناستروزول عبر الجلد كبديل للطريق الفموي. ولذلك، هدفت الدراسة إلى تطوير تركيبة يمكنها التغلب على هذه المشاكل باستخدام مزايا طريق التحريرعبر الجلد ومفاهيم تكنولوجيا النانو. تم صياغةحجم الجسيمات مصغرة ذات إمكانات الزيتا الأعلى من خلال تحضير صيغ الانسترازول النانوسبانلاستك باستخدام طريقة تحديد المستخدم العشوائية لسطح الاستجابة. بالإضافة إلى متغير فئة واحد يتناول نوع منشط الحافة و متغيرين عدديين هوالنسبة الوزنية لمادة السبان٦٠ : منشط الحافة ومدة تشغيل الموجات الفوق الصوتية , وتم اعتبارقياس امكانيات زيتا (ملي فولت) وحجم الجسيمات (نانوميتر) التي تم التحقيق فيها كردود. تم استخدام تقنية التحسين الرياضي للتنبؤ بالقيم المتغيرة المثلى.كشفت التركيبة المحسنة باستخدام نسبة سبان ٦٠ :الصوديوم دي اوكسي كوليت البالغة ١:٩ مع فترة تشغيل الموجات الفوق الصوتية مدتها ٥ دقائق للحصول على حجم جسيمات ١٣٨ نانومترمع امكانيات زيتا تبلغ -٣٢ ملي فولت. تم رؤية الصيغة (عيينة ٢) باستخدام المجهر الإلكتروني النافذ والتي اظهرت شكلا كرويا متجانس ، ونسبة كفاءة الانحباس العالية (٨٠ ٪)، ونمط تحرير لمدة ١٢ ساعة،ومن دراسة التوافق لم تجد اي تفاعل بين الانسترازول والمكونات الاخرى ,تشير النتائج الموصوفة سابقا بأن الأسبانلاستيك قد تكون حاملات دوائية فعالة محتملة لتوصيل الدواء عبر الجلد.

الكلمات المفتاحية: الانسترازول، منشط الحافة، طريقة السطح العشوائية،نانوسبانلاستك،عبر الجلد.